Journal of Inflammation Research

Dovepress
open access to scientific and medical research

Open Access Full Text Article

ORIGINAL RESEARCH

Proteomic and Morphological Profiling of Mice Ocular Tissue During High-altitude Acclimatization Process: An Animal Study at Lhasa

Jun Hou[1,*], Dezhi Zheng[2,*], Xudong Wen[3,*], Wenjing Xiao[4], Fei Han[5], Hongmei Lang[6], Shiqiang Xiong[1], Wei Jiang[5], Yonghe Hu[4], Mengshan He[7], Pan Long[4,5]

[1]Department of Cardiology, Chengdu Third People's Hospital/Affiliated Hospital of Southwest Jiaotong University, Chengdu, People's Republic of China; [2]Department of Cardiovascular Surgery, the 960th Hospital of the PLA Joint Logistic Support Force, Jinan, People's Republic of China; [3]Department of Gastroenterology and Hepatology, Chengdu First People's Hospital, Chengdu, People's Republic of China; [4]School of Materials Science and Engineering, Southwest Jiaotong University, Chengdu, People's Republic of China; [5]Department of Ophthalmology, the General Hospital of Western Theater Command, Chengdu, People's Republic of China; [6]The Center of Obesity and Metabolic Diseases, Department of General Surgery, Chengdu Third People's Hospital & the Affiliated Hospital of Southwest Jiaotong University, Chengdu, People's Republic of China; [7]Department of Pharmacy, Xijing Hospital, Fourth Military Medical University, Xi'an, People's Republic of China

*These authors contributed equally to this work

Correspondence: Pan Long, Department of Ophthalmology, the General Hospital of Western Theater Command, Rongdu Avenue #270, Chengdu, People's Republic of China, Tel +86-181-9125-6132, Email longpan1005@qq.com; Yonghe Hu, School of Materials Science and Engineering, Southwest Jiaotong University, No. 111, North First Section of the Second Ring Road, Chengdu, People's Republic of China, Tel +86-138-8059-6789, Email huyonghe789@sina.com

Purpose: High-altitude environment mainly with hypobaric hypoxia could induce pathological alterations in ocular tissue. Previous studies have mostly focused on sporadic case reports and simulated high-altitude hypoxia experiments. This aim of this study was to explore the proteomic and morphological changes of ocular tissue in mice at real altitude environment.

Methods: In this study, mice were flown from Chengdu (elevation: 500 m) to Lhasa (elevation: 3600 m). After exposure for 1day, 3, 6, 10, 20, 30, and 40days, the mice were euthanatized to obtain blood and ocular tissue. Serological tests, ocular pathological examinations, integral ocular proteomics analysis, and Western blot were conducted.

Results: We focused on acute phase (1–3 days) and chronic phase (>30 days) during high-altitude acclimatization. Serum interleukin-1 was increased at 3 days, while superoxide dismutase, interleukin-6, and tumor necrosis factor-α showed no statistical changes. H&E staining demonstrated that the cornea was edematous at 3 days and exhibited slower proliferation at 30 days. The choroid showed a consistently significant thickening, while there existed no noticeable changes in retinal thickness. Overall, 4073 proteins were identified, among which 71 and 119 proteins were detected to have significant difference at 3 days and 40 days when compared with the control group. Functional enrichment analysis found the differentiated proteins at 3 days exposure functionally related with response to radiation, dephosphorylation, negative regulation of cell adhesion, and erythrocyte homeostasis. Moreover, the differential profiles of the proteins at 40 days exposure exhibited changes of regulation of complement activation, regulation of protein activation cascade, regulation of humoral immune response, second-messenger-mediated signaling, regulation of leukocyte activation, and cellular iron homeostasis. Interestingly, we found the ocular proteins with lactylation modification were increased along high-altitude adaptation.

Conclusion: This is the first work reporting the ocular proteomic and morphological changes at real high-altitude environment. We expect it would deep the understanding of ocular response during altitude acclimatization.

Keywords: altitude response, ocular proteomics analysis, cornea edema, choroid thickening, post-translational modification

Introduction

Apart from the original residents of the plateau for generations, high-altitude (elevation ≥2700 m) environment, with the characteristic of lower barometric pressure, lower temperature, lower ambient humidity, lower oxygen partial pressure and strong radiation is a natural challenge for the human body system, especially for those who rush entry into plateau.[1–3]

Received: 10 February 2022
Accepted: 27 April 2022
Published: 4 May 2022

It may take days, weeks, and even months for people who previously lived at low-altitude to acclimatize to hypobaric hypoxia, thereby acute or chronic high-altitude sickness may occur. It was reported that high altitude induced irreversible/reversible damage to high oxygen and energy demanding tissues like the brain, heart, liver, gastrointestinal tract, as well as ocular system, over a certain period of time.[4–9] The clinical characteristics commonly includes loss of memory function (declined cognitive function), absence of equilibrium function, headache, indigestion, decreased appetite, and so on.[10–13]

In previous studies, much attention has paid on high-altitude pulmonary edema (HAPE) and high-altitude cerebral edema (HACE). They have been demonstrated to be implicated in acute altitude reactions for the reduction of partial oxygen pressure, and the possible mechanism may be related to uneven pulmonary vasoconstriction and disruption of the blood–brain barrier, respectively.[14] However, there is few studies focused on holistic ocular tissue during high-altitude adaptation. And it is unclear whether ocular tissue would develop typical acute and chronic altitude sickness-related symptoms and signs. The eye with its delicate structure and function is always in working condition for receiving light and converting it to an electrical signal and its high precision performance is specifically required for most of the day. It is one of the most metabolically active tissues in the human body. Therefore, it is not surprised that high altitude has both short-term and long-term impact on the eye. Previous clinical observational studies have found retinal hemorrhages, vitreous hemorrhage, papilledema, corneal edema could occur after high-altitude exposure.[3,15]

Moreover, relative clinical reports showed acute altitude sickness (1–3 days) could induce visual disturbances, including visual acuity reduction, intraocular pressure fluctuation, visual field disorder, nerve fiber layer loss, ametropia as well as other pathological changes.[3] The main reasons may be related to retinal blood stagnation and vascular morphology disorder (vascular engorgement and tortuosity). Chronic altitude sickness (>30 days) may cause dry eye, conjunctival degeneration, cataract and other changes, which is probably associated with ultraviolet radiation and hypoxia tolerance.[16–19] Noticeably, previous clinical trials and animal experiments were mostly conducted in the constrained simulating environment with low-pressure and low-oxygen chambers, lacking studies conducted in real high-altitude environment.[20–23] In addition, cell experiments mainly focused on the factor of hypoxia, which could not highlight the systematic influence of high-altitude environment on ocular tissues.[24] Moreover, the molecular cellular stress response and mechanism underlying this pathological process remains unclear during high-altitude acclimatization process.[25] Hence, we systematically explored the pathological impacts of high-altitude hypobaric hypoxic environment on ocular tissues by airlifting mice to Lhasa, Tibet.

In recent years, proteomics and post-translational modification proteomics, employing liquid chromatography-tandem mass spectrometry (LC-MS/MS), have been the popular and promising research field based on the verification of protein structure and function.[26,27] Applying such techniques, researchers can explore the composition, localization, change and interaction of proteins in cells, tissues or organisms, including the protein expression patterns and proteome function patterns.[28] The development of proteomics plays an important role in finding diseases diagnostic biomarkers and toxicological characteristics.[29,30] We used this straightforward method to explore proteomic profiles changes in mice ocular tissue at different time points during high-altitude exposure, which may have great potential to reveal the underlying molecular mechanism of high-altitude influences on the ocular biological structure and function. In terms of hypoxia, a large number of studies have found that oxidative stress, carbon and lipid metabolism, inflammatory, mammalian target of rapamycin (mTOR) and hypoxia-inducible factor (HIF) pathways were complicatedly involved in the regulation of cell homeostasis.[31,32] However, it was still not fully clear whether there existed similar changes at high-altitude adaptation. At present, there is no animal proteomic study elucidating cellular response during a natural high-altitude environment acclimatization, especially on the delicate ocular tissue. At the same time, we studied phosphorylation, lysine crotonylation and lactylation modification in different time periods by pan protein-modified antibody, trying to analyze the cellular stress response in various aspects.

To understand the development and mechanisms of ocular tissue response to high-altitude environment, an integral proteomic analysis and morphological detection were performed in this work. As far as we know, this is the first work that reports on the protein alterations of ocular tissue disorders to high altitude at a proteomic scale. We hope this study will help to achieve a comprehensive understanding of sustained high altitude induced ocular homeostasis.

Methods

Animals

Three hundred and twenty healthy male and 10 female C57BL/6 mice (6–8 weeks of age) were purchased from Chengdu Dossy Experimental Animals Limited in Chengdu, China (License No. SCXK20 20–030). Three hundred male C57BL/6 mice were airlifted from Chengdu (elevation of 500 m) to Lhasa (elevation of 3600 m) in July, 2020 and housed in Tibet autonomous Region Key Laboratory of Veterinary Drugs of Tibet Vocational Technical College. The housing environments were: atmospheric pressure, 65.20±0.05 kPa; temperature, nighttime, 12±5°C, daytime, 18±5°C; humidity <20%; natural light irradiation. Twenty healthy male and 10 female C57BL/6 mice were housed in Chengdu under standard laboratory conditions. The housing environments were: atmospheric pressure, 94.50±0.05 kPa; temperature, 23±3°C; humidity, 50±10%; natural light irradiation. All experiments were performed in compliance with the Association for Research in Vision and Ophthalmology (ARVO) Statement for the Use of Animals in Ophthalmic and Vision Research. Studies were approved by the research ethics committee for care and use of laboratory animals at the General Hospital of Western Theater Command.

Blood and Tissue Collection

Mice were euthanatized with lethal dose of pentobarbital sodium (Sigma-Aldrich Co., St Louis, MO, USA) by intraperitoneal injection at 1day (D1), 3 (D3), 6 (D6), 10 (D10), 20 (D20), 30 (D30), and 40days (D40) post high-altitude exposure. The operation procedures were as follows. The mice were weighed and their limbs were expanded and fixed after the injection of excessive anesthetic. Then, the right atrial appendage was quickly cut after the thoracotomy, and the non-anticoagulation tube was used to collect 100–200 μL cardiac blood. One half of mice in each group underwent cardiac perfusion with icy normal saline using a blunt needle which inserted into the left ventricle for about 50–100 mL perfusion. The other half were fixed with 4% paraformaldehyde solution and stopped after limb stiffness, about 40–60 mL formaldehyde solution. All operations are performed by two skilled animal anatomy technicians. Eyeball (connected with the optic nerve about 1–2 mm), brain tissues (hippocampus, striatum, cerebellum and cortex were collected, separately), heart, lung, liver, kidney, and testicle were removed successfully. The proteinsamples were collected in centrifugal tubes with liquid nitrogen cryopreservation and then transferred to a −80°C refrigerator. Thepathological samples were fixed in 4% paraformaldehyde and stored at room temperature, and the eyeballs were specially fixed with dedicated eyeball fixed liquid. The corresponding lowland mice, as control group (D0), were disposed with the same method. The collected blood was centrifuged at 1200 g for 10 min at 4°C to obtain serum for subsequent detection of inflammation and oxidative stress related factors. All protein tissues were sent to Chengdu in four batches with abundant dry ice, and then sent to Hangzhou Jingjie Biological Co., Ltd for proteomic testing. The pathological samples were sent to Chengdu laboratory for pathologically histological analysis after careful examination.

Histological Analysis

Eyeballs were fixed in dedicated eyeball fixed liquid (glacial acetic acid: formaldehyde: normal saline: ethyl alcohol=1:2:7:10) for at least 48 h. After gradient ethanol dehydration, paraffin embedding and other traditional sample disposal processes as previously described,[33,34] 4 micron (μm) sections were cut through optic nerve in sagittal position. Then the sections were baked and dewaxed before hematoxylin and eosin (H&E) staining. After vitrification by dimethylbenzene and sealing by resinene, H&E staining sections were scanned with NanoZoomer Digital Pathology System (Hamamatsu Photonics Co., Ltd) and viewed with NDP view software. Then the thickness of cornea, retina and choroid were measured. The description of corneal thickness was from corneal epithelium layer to endothelial layer, and retinal thickness was from retinal internal limiting membranes to pigment epithelium layer. As for choroid thickness, it was from Bruch's membrane (connected with retinal pigment epithelium layer) to sub-choroid space (attached to the sclera).

Serum ELISA Detections

The mice serum samples were collected as described (in "Blood and tissue collection" section). Fifteen serum samples of each group, including D1, D3, D6, D10, D20, D30, and D40 post high-altitude (3600 m) exposure and

Control group (D0) at low-altitude (500 m) were assessed by commercially available mouse enzyme-linked immunosorbent assay (ELISA) kit from JianCheng Bio-tech Co., Ltd (Nanjing, China) according to the manufacturer's instructions.[35]

Sample Preparation for MS

The cryopreserved ocular tissue was fully ground to powder with liquid nitrogen in a precooled mortar. The crushed sample was placed in cracking buffer (8 M urea; Sigma, USA), 1% protease inhibitor; Calbiochem, USA) and immediately homogenized. Debris was pelleted in centrifuge at 12,000 g for 10 min at 4°C, and supernatant was transferred to a new tube. Bicinchoninic acid (BCA) kit (Thermo Fisher Scientific, Waltham, MA, USA) was used for protein concentration determination. The sample solution was reduced with 5 mM dithiothreitol (DTT) at 56°C for 30 min, and then alkylated with 11 mM iodine acetamide (IAA) for 15 min at room temperature avoiding light. The final urea concentration in the protein sample was reduced to less than 2 M. The protein was overnight digested by trypsin (Promega, Fitchburg, WI, USA) with a protein-to-trypsin ratio of 50:1 at 37°C.

LC-MS/MS Analysis for Protein Identification

An ultra-high performance liquid chromatography (UPLC) system EASY-nLC 1200 (Thermo Fisher Scientific) was coupled online to a quadrupole Orbitrap Exploris™ 480 mass spectrometer with a nano-electrospray ion source for the analysis of eye tissue proteome. The peptides were dissolved by solvent A (0.1% formic acid and 2% acetonitrile in water), and loaded onto the nanoscale C18-reversed phase HPLC-column with solvent A and separated with an 86-min gradient of 6–80% solvent B (90% acetonitrile and 0.1% formic acid in water) at a constant flow rate of 500 nL/min. The total duration of the run was 90 min. The ion source voltage was 2.3 kV. The dynamic exclusion duration of data-dependent MS/MS acquisition was 20 seconds for peptides analyses avoiding repeated scanning of parent ions. High resolution Orbitrap was applied for the detection and analysis of peptide parent ions and their secondary fragments. In first-level mass spectrometry, the resolution was 60,000 with the scanning range of 400–1,500 m/z. In secondary mass spectrometry, the resolution was 15,000 with the scanning range of 110 m/z, and TurboTMT was set as off. The 25 most signal intensive precursor ions were selected for tandem mass spectrometry (MS/MS) analysis. MaxQuant computational platform (v1.6.15.0; Max Planck Institute of Biochemistry, Martinsried, Germany) was applied to process the MS data according to the quantitative parameters of the 4D label-free analysis. The integrated Andromeda search engine was used for peptides and proteins identification at a false discovery rate (FDR) of less than 1%. The data were searched through the human Universal Protein Resource (UniProt, https://www.uniprot.org/) database (downloaded November, 2017) to match with known proteins.[36]

Bioinformatics Analysis

To explore the cellular component, molecular function, and biological process of the tremendous genes and classify functionally associated genes/terms into a manageable number of biological modules in a network context, Gene Ontology (GO) annotation, and Visualization and Integrated Discovery (DAVID) bioinformatics resources (http://david.ncifcrf.gov) were applied.[37,38] Pathway attribution analysis was accomplished by using Kyoto Encyclopedia of Genes and Genomes (KEGG) database (https://www.kegg.jp/). Molecular interaction networks of the identified proteins were obtained by employing STRING analysis software (http://string-db.org/).[39,40] Moreover, Heatmap and Venn diagram were accomplished by TB tool software.[41] In order to illustrate the temporal proteomic profiling of ocular tissue during high-altitude adaptation, the bioinformatics analysis was conducted at each time point comparing the Control eyes.

Immunoblotting Detections

Whole eyeballs were dissected and protein was isolated as described previously.[42] Sodium dodecyl sulfate-polyacrylamide gel electrophoresis (SDS-PAGE) of total eyeballs proteins were performed with Tris-glycine-SDS running buffer. Then the gels were stained with coomassie brilliant blue. Next, the proteins from the gels were transferred onto nitrocellulose filter membrane (Bio-Rad Laboratories, Germany) with electroblotting. After blocking with 5% nonfat milk solution, membranes were incubated with pan phosphorylation antibody, pan lactylation antibody and pan

lysine crotonylation antibody (PTM BioLab, China) overnight at 4°C. Binding of HRP-conjugated secondary antibody (Thermo Fisher Scientific) was observed using enhanced chemiluminescence (Thermo Fisher Scientific). All blots were quantified by densitometry using Image J software (NIH).

Statistical Analysis

The data were analyzed and visualized with Statistical Product and Service Solutions (SPSS) 25.0 software (IBM Corporation, Armonk, NY, USA) and GraphPad Prism 8.0 (San Diego, CA, USA). To compare the differences among the groups, one-way analysis of variance (ANOVA) was used for normally distributed data, whereas the Kruskal–Wallis test was used for non-normally distributed data. A P-value <0.05 indicated a significant difference.

Results

Overall Design Flow Chart of Experiment

To explore the ocular tissue adaptation characteristics on real high-altitude environment, we designed this animal experiment. Mice living in low-altitude for generations were flown from lowland (Chengdu, elevation: 500m) to high altitude (Lhasa, elevation: 3600m) in short period (flight time: two hours). As shown in Figure 1, to thoroughly study the structure and biological molecular manifestation of ocular tissue, we selected seven time points (D1, D3, D6, D10, D20, D30, and D40) post high-altitude arrival to study. In these seven time points, we observed the physical condition of the mice, including body weight, motion ability, and ocular characteristics. Moreover, we collected serum, ocular tissue (including total eyeball with 1–2mm optic nerve, except ocular adnexal), and other organs. We regarded D1 to D3 as acute high-altitude phase and D30 to D40 as chronic high-altitude phase according to previous references.[3] We prepared serum samples and entire eyeball tissues from each time points for pathological and proteomic analyzation. Three eyeball samples (single eye) randomly acquired from the mice at D1, D3, D6, D10, D20, D30, and D40 post high-altitude and D0 (Control) were selected to perform label-free LC-MS/MS.

Body Weight Loss During Acute High-altitude Exposure

As we know, an overall manifestation of the cellular stress response is weight loss. In Figure 2, we tested the body weight of the mice at seven time points post high-altitude exposure. To our surprise, their body weight at D3 was 16.35±1.12 g, which was significantly less than that in Control (18.30±0.69 g) (P<0.05). However, there existed no significant difference between D1 and Con (P>0.05). When it came to D6, the body weight of the mice increased continually. Moreover, we did not compare the corresponding body weight of low-altitude mice because the purpose of this study was mainly to determine whether hypobaric hypoxia influenced basic physical conditions. In addition, qualitative observation

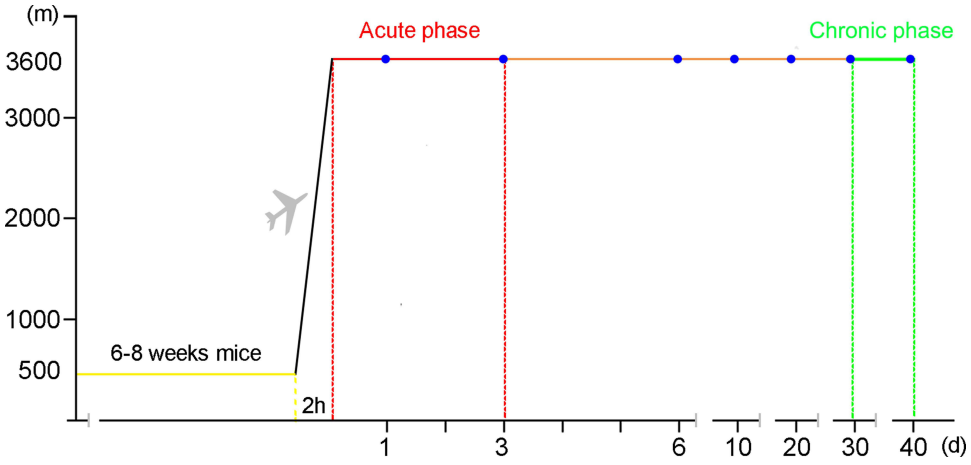

Figure 1 Overall design flow chart of experiment.

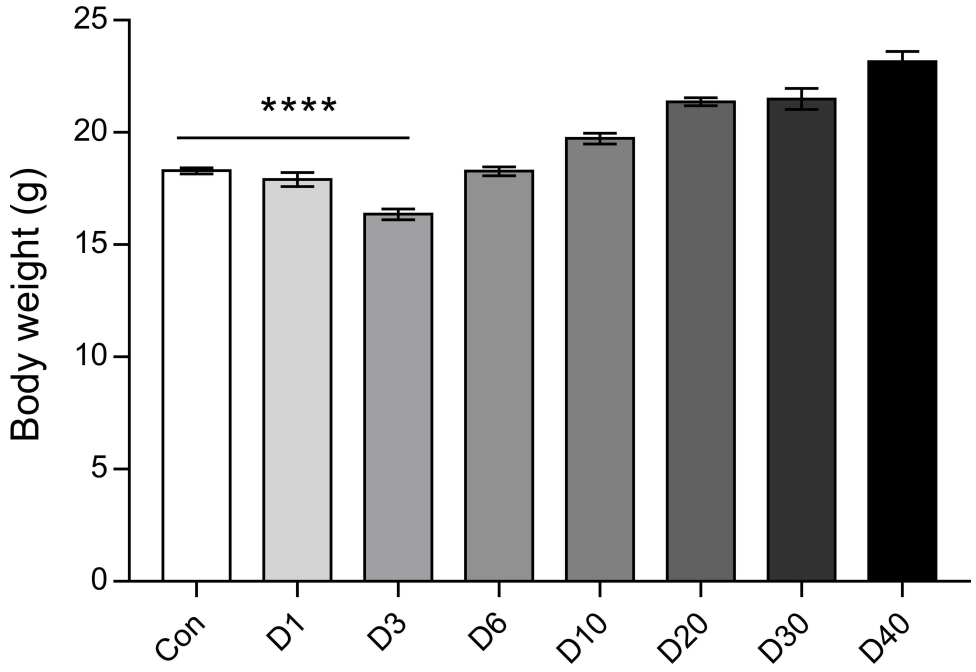

Figure 2 The body weight of mice at D0 (Control), D1, D3, D6, D10, D20, D30, and D40 post high-altitude adaptation. Values are presented as mean ±SD, N=15-30. ****P<0.0001: D1 group, D3 group, D6 group, D10 group, D20 group, D30 group, and D40 group vs Control (D0) group.

found the motion ability of the mice at D1 and D3 post high-altitude exposure tended to decline manifested by reduced spontaneous activities.

Serum Inflammation Stress Increasing During Acute High-altitude Exposure

To evaluate serum inflammation stress-related factors, we detected serum IL-1, IL-6, TNF-α, and SOD. As shown in Figure 3A, the serum level of IL-1 at D3 and D6 was 98.67±12.31 pg/mL and 90.33±11.90 pg/mL, which was both significantly more than that (57.54±14.55 pg/mL) at D0 (Control) (all P<0.05). As for IL-6 (Figure 3B) and SOD (Figure 3C), we found both an obvious peak at D3, although there existed no statistical difference among those detecting time (all P>0.05). Moreover, the serum level of TNF-α (Figure 3D) was relatively stable at each detecting time points.

The Morphological Changes of Cornea, Retina and Choroid During High-altitude Exposure

It was a controversial issue that the high-altitude effects on pathology structure of ocular tissue. We applied H&E staining to explore the potential changes of ocular tissue during high-altitude exposure. As shown in Figure 4A, we focused on the cornea, retina and choroid morphological changes and the thickness was calculated by NDP view software with the average value of several sites (Supplement Figure 1).

As shown in Figure 4B, corneal edema occurred at D1 (140.67±9.12 μm) and D3 (154.33±7.82 μm) post high-altitude exposure compared with that at D0 (123.83±5.61 μm) which mainly manifested by the stromal layer edema (all P<0.05). Then, it showed a gradual alleviation of corneal edema at later acclimatation (D6 and D10). However, when it came to D20 (110.83±8.25 μm), D30 (112.67±7.93 μm) and D40 (106.00±6.51 μm) post high-altitude adaptation, the trend of corneal thinning was found, and this could have resulted from the decreased proliferation of corneal epithelium cells.

As shown in Figure 4C, the holistic retinal structural changes did not reach the scale of statistically significant difference, although an increase of retinal thickness was showed at D30 (209±6.43 μm) and D40 (215.50±9.27 μm). However, we were not sure whether this was a manifestation of retina edema or a developing issue.

In the aspect of choroid, the data in Figure 4D revealed a noticeable thickening trend during high-altitude adaptation. In initial stage, the thickness of choroid at D6 (26.14±1.90 μm) significantly increased compared with that at D0 (21.53

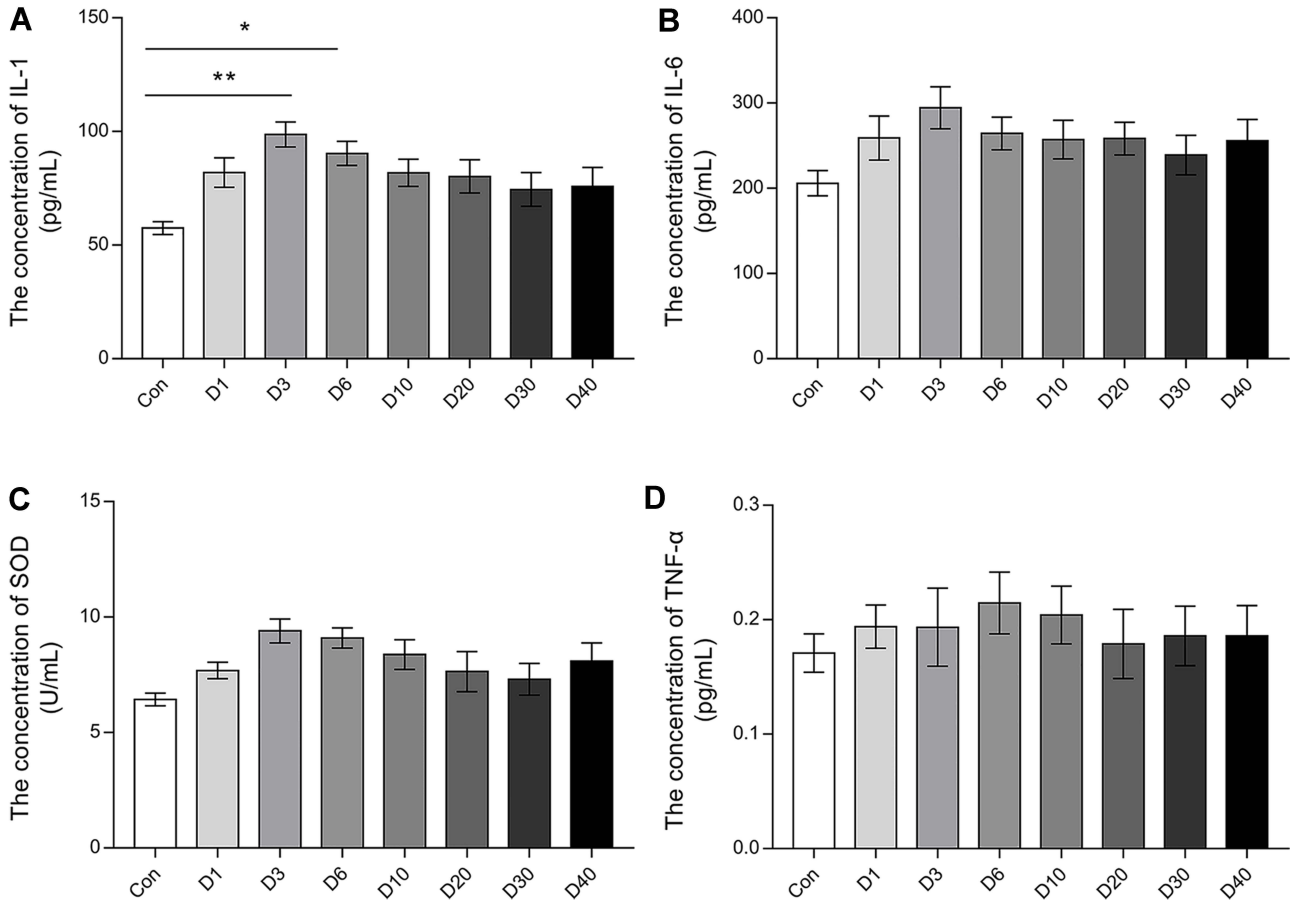

Figure 3 The serum inflammation stress related factors of mice at D0 (Control), D1, D3, D6, D10, D20, D30 and D40 post high-altitude adaptation. (**A**) The level of serum IL-1. (**B**) The level of serum IL-6. (**C**) The level of serum SOD. (**D**) The level of serum TNF-α. Values are presented as mean ±SD, N=15. **P*<0.05, ***P*<0.01: D1 group, D3 group, D6 group, D10 group, D20 group, D30 group, and D40 group vs Control (D0) group.

±2.55 μm) (*P*<0.05). Then, choroid thickness was continuedly increased at D10 (26.53±2.01 μm), D20 (27.67±1.32 μm), D30 (28.31±1.14 μm), and D40 (29.53±2.73 μm), and we suspected that it may be attributed to the choroidal vessel's stasis and slowed venous return.

Quantitative Proteomic Characteristic of Ocular Tissue During High-altitude Exposure

As shown in Figure 5A, liquid chromatography mass spectrometry (LC-MS) identified 2,594,454 secondary spectra, and there were 870,853 (spectrum utilization rate was 33.6%) availably matched spectra. Spectral analysis based on Proteome Discoverer database recognized 29,605 peptides, of which 28,331 were specific peptides. Fortunately, among 4,073 identified proteins, 3403 were quantified. MS data quality control including peptides length and amount distribution and proteins coverage and molecular weight distribution. Proteins were identified and quantified using MaxQuant with the following criteria: (i) at least one peptide per protein identified; (ii) protein detected in at least 1/5 experiments.

Figure 5B showed that the most of proteins coverage was below 30%, which indicated the protein abundance was suitable. Meanwhile, for biological or technical duplicate samples, it is necessary to test whether the quantitative results of biological or technical duplicate samples conform to statistical consistency. Three statistical analysis methods, including Pearson's correlation coefficient (PCC) (Supplement Figure 2), principal component analysis (PCA), and relative standard deviation (RSD) (Supplement Figure 3) were used to evaluate repeatability. All those statistical methods showed a favorable biological or technical accuracy and reproducibility. Moreover, the PCAdemonstrated a clear

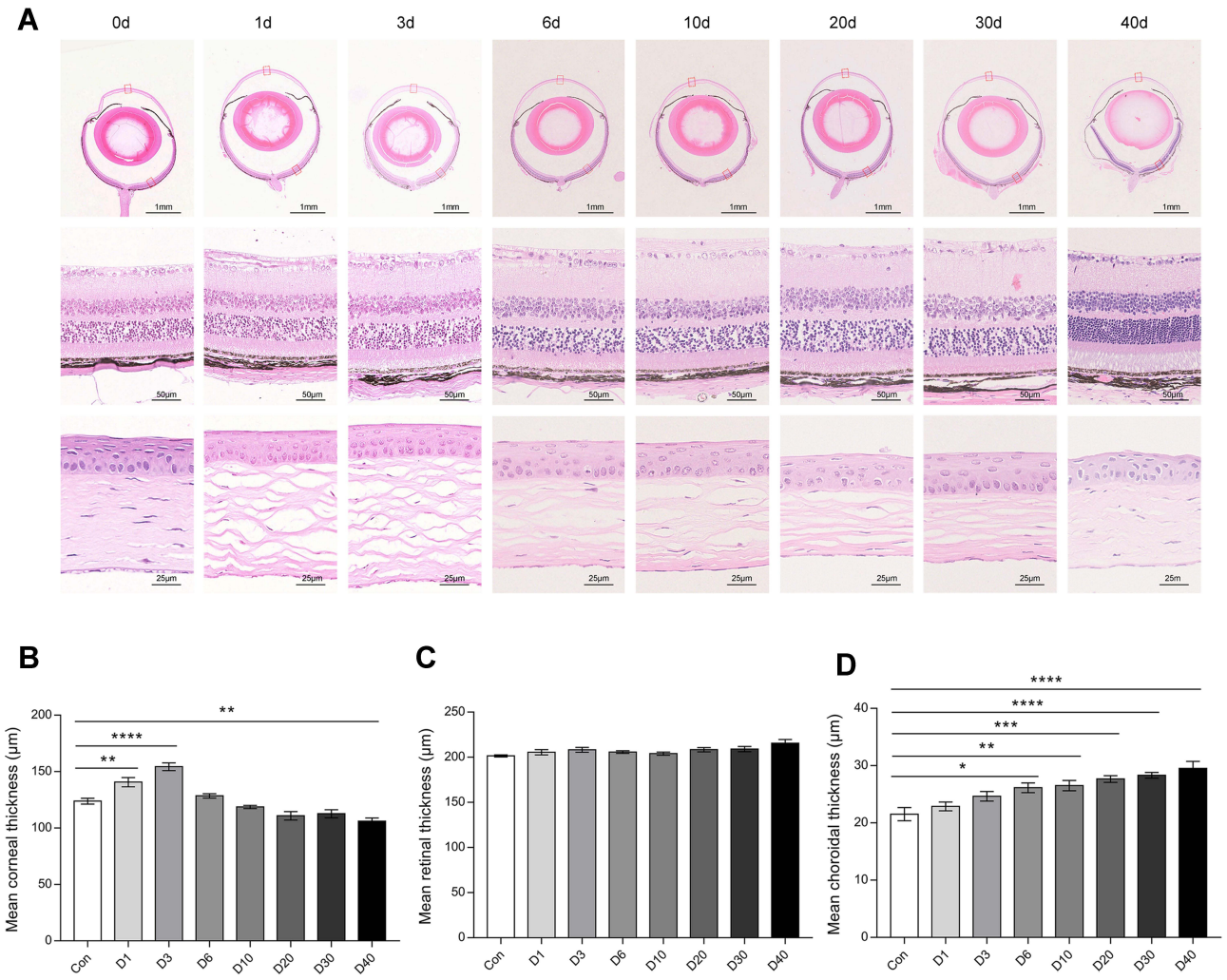

Figure 4 The morphological changes of ocular tissue at D0 (Con), D1, D3, D6, D10, D20, D30 and D40 post high-altitude adaptation. (**A**) Representative H&E staining picture of ocular tissues (cornea, retina, and choroid). (**B**) The mean thickness of cornea. (**C**) The mean thickness of retina. (**D**) The mean thickness of choroid. Scale bar = 1000/50/25 μm; Values are presented as mean ±SD, N=6. **P*<0.05, ***P*<0.01, ****P*<0.001, *****P*<0.0001: D1 group, D3 group, D6 group, D10 group, D20 group, D30 group, and D40 group vs Control (D0) group.

separation of protein signatures at different high-altitude acclimatation time and confirmed high-quality proteins data for further functional analysis (Figure 5C).

This study considered 1.2-fold change as the threshold of differential abundance change, and a *P*-value <0.05 as the threshold of statistical significance. Figure 5D showed the number of differential proteins in D1, D3, D6, D10, D20, D30, and D40 post high-altitude compared with D0, respectively. Among the 3403 quantified proteins, differential protein analysis found 97 proteins were determined be upregulated (D3 vs Control, fold change >1.2, *P*<0.05), and 91 proteins were identified be downregulated (D3 vs Control, fold change <0.833, *P*<0.05). At D40 post high-altitude exposure, 180 proteins were upregulated (fold change >1.2, *P*<0.05), and 179 proteins were downregulated (fold change <0.833, *P*<0.05).

The Protein Profile Changes of Ocular Tissue During Acute High-altitude Exposure

To determine the effect of acute high-altitude response on ocular tissue, we analyzed the protein profile at D3 post high-altitude exposure. The representative upregulation and downregulation proteins (fold change >2, *P*<0.05) were shown in Figure 6A and 6B. In addition, we conducted enrichment analysis at Gene Ontology (GO) classification for differentially expressed proteins in each comparison group (Fisher's exact test is used here to calculate significance *P*-value).

A

Title	Number
Total spectrums	2594454
Matched spectrums	870853
Peptides	29605
Unique peptides	28331
Identified proteins	4073
Quantifiable proteins	3403

B

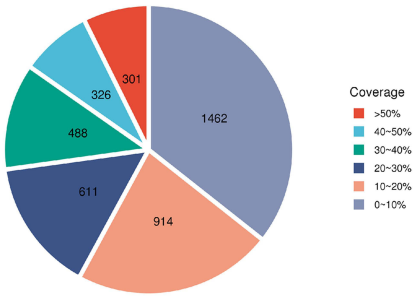

C

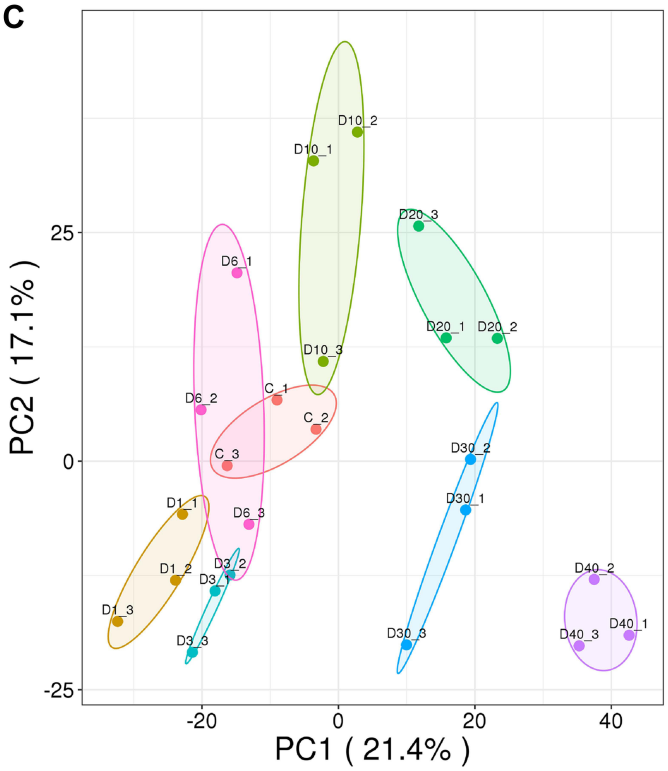

D

Compare group	Regulated type	fold change >1.2	fold change >1.3	fold change >1.5	fold change >2
D1/C	Upregulated	78	62	33	6
	Downregulated	66	45	28	11
D3/C	Upregulated	97	69	28	8
	Downregulated	91	66	43	20
D6/C	Upregulated	93	59	30	8
	Downregulated	131	91	55	22
D10/C	Upregulated	84	48	24	9
	Downregulated	93	69	40	15
D20/C	Upregulated	101	57	21	6
	Downregulated	105	74	37	13
D30/C	Upregulated	146	80	32	6
	Downregulated	154	113	65	27
D40/C	Upregulated	180	116	52	10
	Downregulated	179	127	67	17

Figure 5 Basic information of quantitative proteomics of ocular tissue at D0 (Control), D1, D3, D6, D10, D20, D30, and D40 post high-altitude adaptation. (**A**) Total mass spectrometry data. (**B**) The coverage rate of identified protein. (**C**) The principal component analysis (PCA) of protein quantification among different groups. (**D**) Quantitative proteomics identification of differentially abundant proteins with the different fold change at D0 (Control), D1, D3, D6, D10, D20, D30, and D40 post high-altitude adaptation.

Commonly, GO terms focused on biological process (BP), cellular component (CC), and molecular function (MF). In this study, we paid attention on BP to explore how cell stress response changed to acute high-altitude response. As shown in Figure 6C, the bubble diagram found the functions of upregulation protein profile (D3 vs Control) were mainly concentrated on cellular response to stimulate light, response to UV, and response to radiation. As for the downregulation protein profile, the function mainly enriched on dephosphorylation, negative regulation of cell adhesion, and erythrocyte homeostasis pathways (Figure 6D).

The Protein Profile Changes of Ocular Tissue During Chronic High-altitude Exposure

To determine the effect of chronic high-altitude response on ocular tissue, we analyzed the protein profile expression at D40 post high-altitude adaptation. The representative upregulation and downregulation proteins (fold change >2, $P<0.05$) were shown in Figure 7A and 7B. In addition, we conducted enrichment analysis at GO classification for differentially expressed proteins in each group. In this study, functional enrichment analysis was conducted to demonstrate the specific mechanism of cell stress response to chronic high-altitude response. As shown in Figure 7C, the bubble diagram found the functions of upregulation protein profile (D40 vs Control) were mainly centralized on regulation of complement activation, regulation of protein activation cascade, regulation of humoral immune response, cellular response to dsRNA, second-messenger-mediated signaling, regulation of leukocyte activation, cellular iron homeostasis, iron homeostasis, and cellular chemical homeostasis. As for the downregulation protein profile, the function mainly enriched on regulation of lipid metabolic process pathways (Figure 7D).

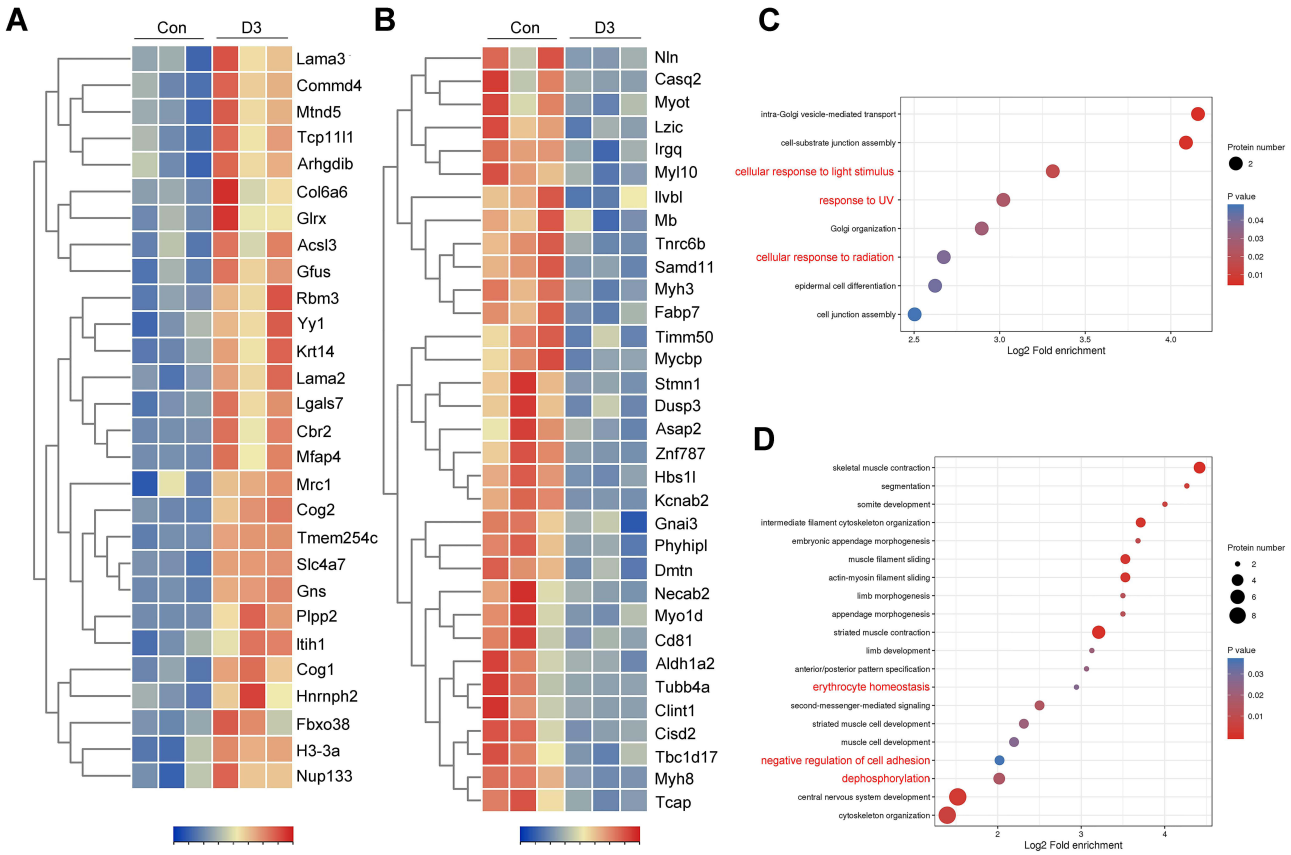

Figure 6 The protein profile changes of ocular tissue during acute high-altitude exposure. (**A**) The relative expression of upregulation protein profiles at D3 post high-altitude adaptation compared with D0 (Control) shown by heatmap. (**B**) The relative expression of downregulation protein profiles at D3 post high-altitude adaptation compared with D0 (Control) shown by heatmap. (**C**) The bubble diagram of the upregulation protein profiles functional enrichment analysis focus on biological process. (**D**) The bubble diagram of the downregulation protein profiles functional enrichment analysis focus on biological process. For hierarchical row clustering protein data was scaled normalization. Red cell color indicates an upregulation, navy blue cell color indicates a downregulation. The respective color code is given above each heat map. The color of the circle indicated the enrichment significance *P*-value, and the size of the circle indicated the number of differential proteins in the functional class or pathway.

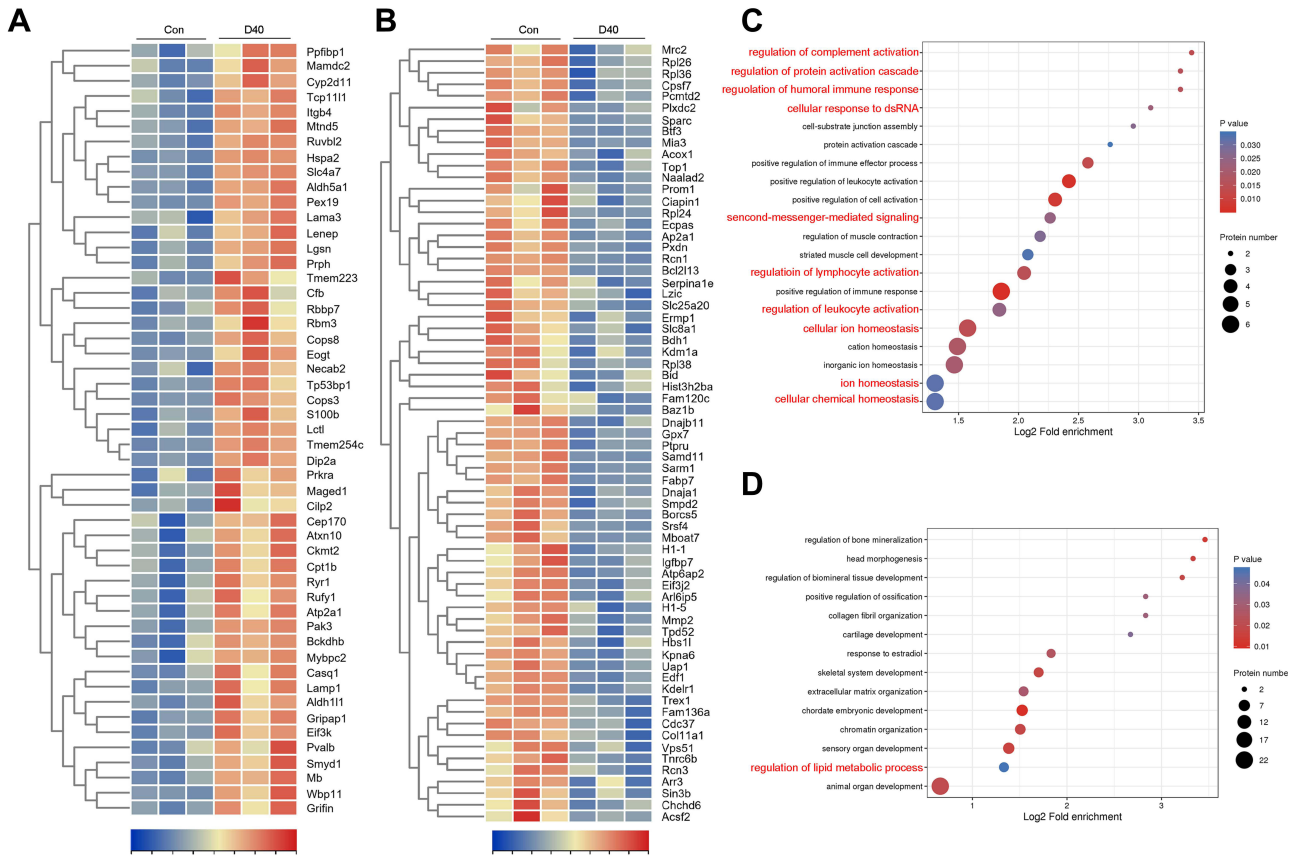

Figure 7 The protein profile changes of ocular tissue during chronic high-altitude exposure. (**A**) The relative expression of upregulation protein profiles at D40 post high-altitude adaptation compared with D0 (Control) shown by heatmap. (**B**) The relative expression of downregulation protein profiles at D40 post high-altitude adaptation compared with D0 (Control) shown by heatmap. (**C**) The bubble diagram of the upregulation protein profiles functional enrichment analysis focus on biological process. (**D**) The bubble diagram of the downregulation protein profiles functional enrichment analysis focus on biological process. For hierarchical row clustering protein data was scaled normalization. Red cell color indicates an upregulation, navy blue cell color indicates a downregulation. The respective color code is given above each heat map. The color of the circle indicated the enrichment significance *P*-value, and the size of the circle indicated the number of differential proteins in the functional class or pathway.

The Differential Protein Profile Between Acute and Chronic High-altitude Exposure

In order to determine the different effects of acute high-altitude response and chronic high-altitude response on ocular tissue, we analyzed the protein profile changes at D3 and D40 post high-altitude exposure. As shown in Figure 8A, 14 overlap differential proteins (Venn diagram) were found at D3 and D40 post high-altitude acclimatization compared with D0. The volcano plot showed 96 upregulation proteins and 74 downregulation proteins at D40 compared with those at D3 (Figure 8B). The representative upregulation and downregulation proteins (fold change >2, $P<0.05$) shown in Supplement Table 1. Moreover, a subcellular structure annotation (Figure 8C) found 170 differential proteins (D40 vs D3) positioned mainly in cytoplasm (30.59%), nucleus (21.76%), and mitochondria (13.53%). Meanwhile, 170 differential proteins were applied with GO analysis for three aspects (BP, CC, and MF). Figure 8D showed there existed 85 proteins functioned with "response to stimulus" of total differential proteins. In order to determine the differential cell stress response effects of acute high-altitude response and chronic high-altitude response on ocular tissue, we analyzed the stimulation response protein profile at D3 and D40 post high-altitude adaptation. Forty-seven upregulation and 38 downregulation proteins were shown in Figure 9A with heatmap. Moreover, based on the STRING database (STRING: functional protein association networks; https://string-db.org/), protein–protein interaction (PPI) networks of the differentially expressed proteins functioned with cell stress response were constructed (Figure 9B). PPI network featured 85 uniquely expressed nodes and 124 edges (52 expected number of edges). Furthermore, the results found those 85 cell response proteins were participated in metabolic pathway (SIRT), glutathione metabolism pathway (GST), and

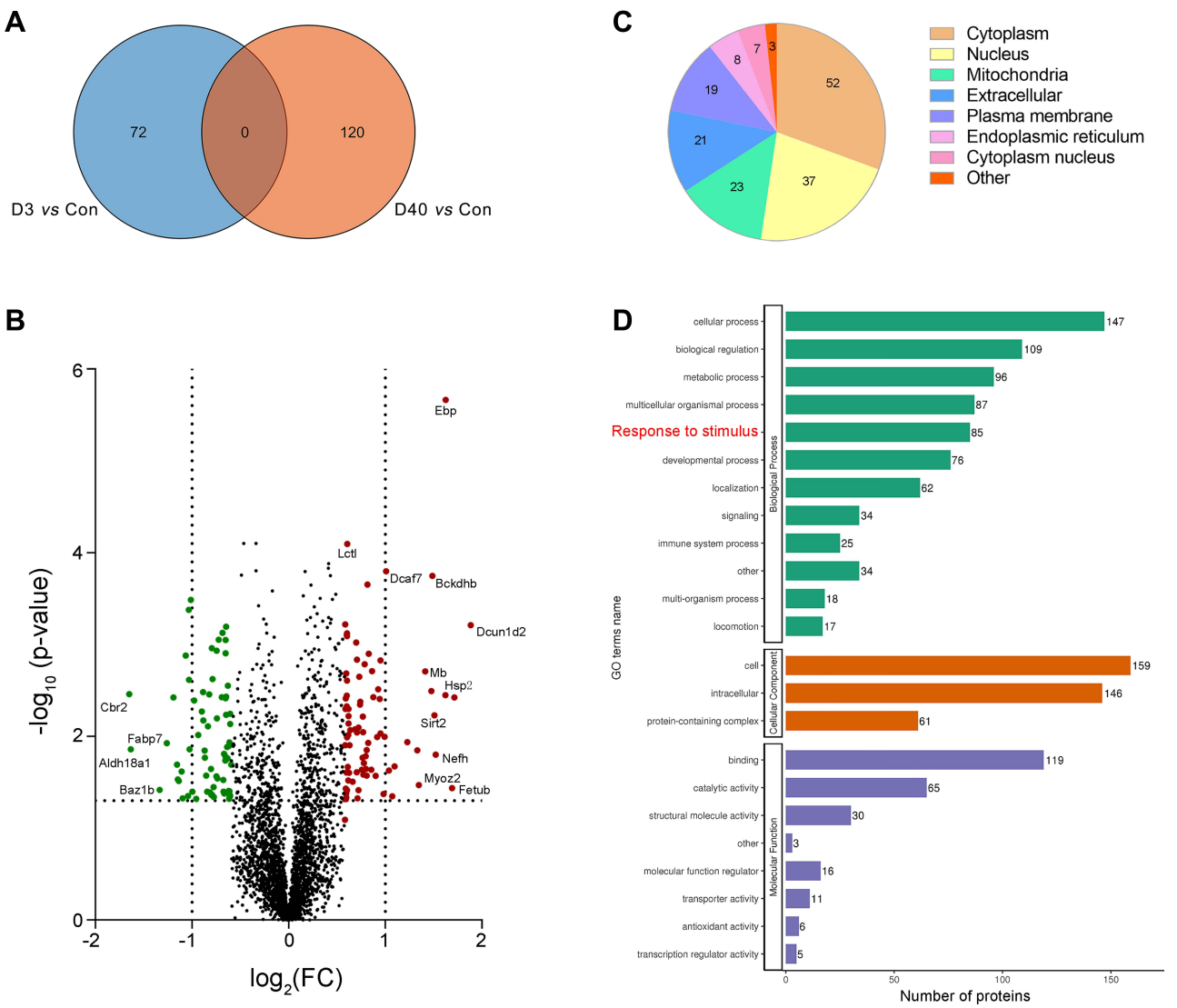

Figure 8 A comparison of ocular tissue proteomic profiles between acute and chronic high-altitude process. (**A**) Venn diagram showing the overlap of the significantly regulated proteins following 3 days (D3) and 40 days (D40) post high-altitude acclimatization process. (**B**) Volcano plot showing the differential protein profile between D3 and D40. (**C**) Subcellular structure annotation of the significantly regulated proteins at D3 and D40. (**D**) The number of differential proteins based on GO analysis between D3 and D40 post high-altitude exposure.

ferroptosis pathway (GPX7). Therefore, we concluded that cell metabolism could play a prominent role in cell response on acute or chronic high-altitude exposure.

Dynamic Expression Profile of Ocular Tissue Proteins During High-altitude Exposure

As we know, high-altitude environment with hypobaric hypoxia, low temperature, low humidity, and high ultraviolet light could result in a series of cellular stress responses. Oxidative stress, ferroptosis, apoptosis, autophagy, endoplasmic reticulum stress (ERS) and so on are wildly and extensively studied in many kinds of diseases. Therefore, as shown in Figure 10, we analyzed the key components or regulation proteins of oxidative stress and ferroptosis pathways. Figure 10A showed that the proteins, such as superoxide dismutase 1 (SOD1), superoxide dismutase 2 (SOD2), glutathione peroxidase (GPX) family, and catalase (Cat), which participated in anti-oxidative cellular stress process, were dramatically increased at D30 and D40 post high-altitude acclimatization (black rectangle). However, oxidative stress proteins, including interleukin enhancer-binding factor 2 (ILf2) and interleukin enhancer-binding factor 3 (ILf3) showed a slighter fluctuation among high-altitude adaptation. Additionally, we found ferroptosis related proteins

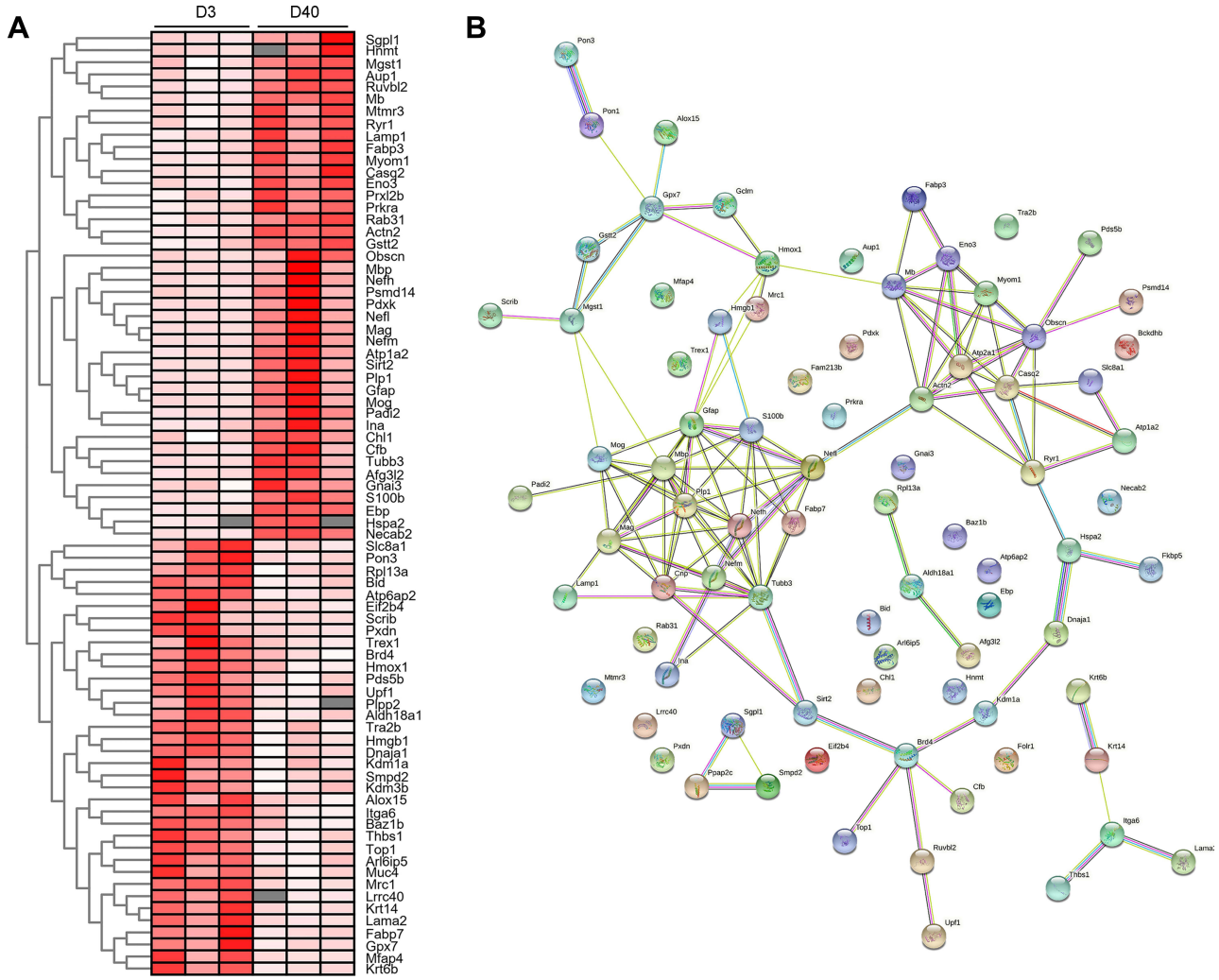

Figure 9 The analysis of cell response related proteins between acute and chronic high-altitude process. (**A**) The relative expression of differential protein profiles concerning cell stress response at D40 post high-altitude adaptation compared with D3 shown by heatmap. (**B**) PPI analysis of cell response related proteins between D3 and D40 post high-altitude exposure. For hierarchical row clustering protein data was log2 transformed. Red cell color indicates an upregulation, white cell color a downregulation. The respective color code is given above each heat map.

transferrin receptor protein 1 (Fth1), cysteine desulfurase (Nfs1), CDGSH iron-sulfur domain-containing protein (Cisd2 and Cisd3) and, serotransferrin (Tf) were increased post 10 days of high-altitude adaptation (Figure 10B, blue rectangle). Moreover, heme oxygenase 1 (Hmox1), nuclear receptor coactivator 5 (Ncoa5), and Cisd1 expressions were enhanced at D3 and weakened at D20 to base level post high-altitude exposure (purple rectangle).

The Post-translational Modification of Ocular Tissue During High-altitude Exposure

As we all know, not only could the quantity of proteins modulate cell conditions, but also the quality of proteins could affect cell ability. Post-translational modification (PTM) is a vital way to regulate protein structures and functions, which attracted researcher's attentions. Therefore, we applied Western blot detection to evaluate the level of proteins with lysine crotonylation modification, phosphorylation modification, and lactylation modification. As shown in Figure 11A, we detected the level of PTMs at D0 (Control, Male), D0 (Control, Female), D1, D3, D6, D10, D20, D30, and D40 post high-altitude exposure. Coomassie bright blue staining found each sample protein was equal and the molecular weight of proteins were concentrated between 15–25 kD (Figure 11B). As shown in Figure 11C and D, lysine crotonylation modification mainly expressed at the protein molecular weight of 55kD, 25kD, and 20kD. Moreover, we found that lysine crotonylation modification was decreased at D3 and increased at D20 post high-altitude adaptation. In addition,

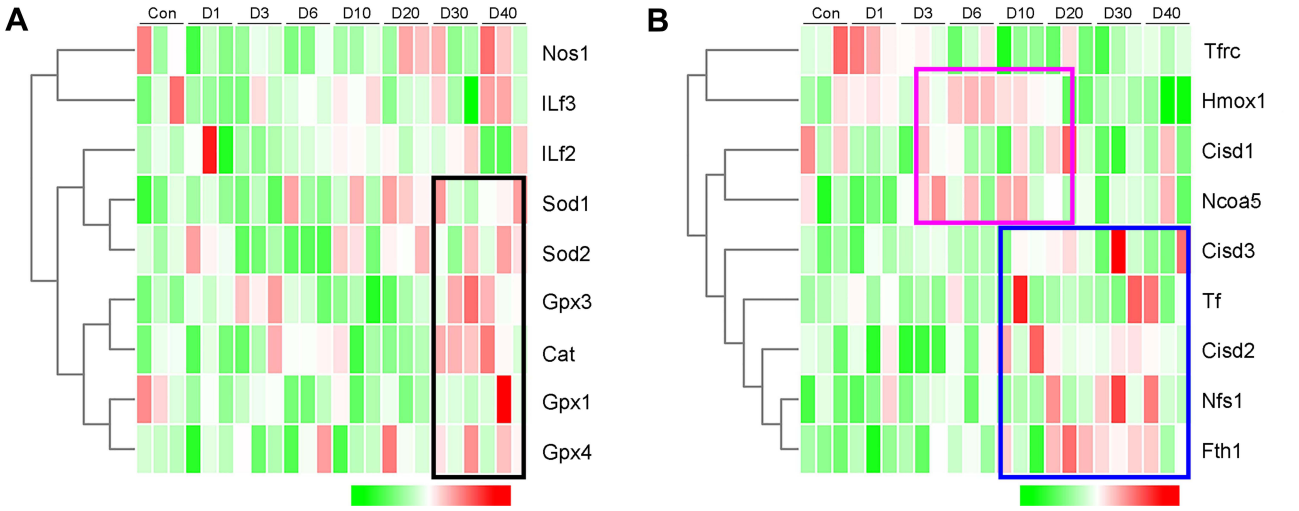

Figure 10 The expression analysis of proteins assigned to the clusters linked with oxidative stress and ferroptosis at D0 (Control), D1, D3, D6, D10, D20, D30, and D40 post high-altitude adaptation. (**A**) The relative expression of oxidative stress related protein cluster. (**B**) The relative expression of ferroptosis related protein cluster. For hierarchical row clustering protein data was scaled normalization. Red cell color indicates an upregulation, green cell color a downregulation. The respective color code is given above each heat map. The black, blue, and purple rectangle showed an increased tendency.

Figure 11E and F found that phosphorylation modification mainly expressed at the protein molecular weight of 15kD and 20kD. Meantime, we found that phosphorylation modification showed no obvious changes during high-altitude adaptation. Furthermore, Figure 11G and H demonstrated that lactylation modification mainly expressed at the protein molecular weight of 25kD. Interestingly, we found that lactylation modification was increased along with high-altitude adaptation.

Discussion

We explored the ocular changes during high-altitude acclimatization process in diversified parts, including systematic level test, ocular morphological characteristics, and ocular proteomic profiling study. Our results provided comprehensive and valuable evidence regarding the time course patterns of ocular acclimatization to high altitude. The acute phase (1–3 days) was manifested with body weight loss, corneal edema, and protein profiles of response to UV radiation and erythrocyte homeostasis increasing. The chronic phase (>30 days) was characterized by choroid thickening, corneal proliferation decreasing and protein profiles of oxidative stress, ferroptosis, and response to immunoregulation increasing.

High-altitude environment is complicated and hostile, it is a great challenge for those who rush entry into plateau from lowland.[43] As we know that body weight reflected the total stress level of the body,[44] we found an obvious body weight decreasing in mice at the acute phase of 3 days exposure. As for the components of the ocular tissue, we focused on the morphological changes of cornea, retina and choroid. The cornea is located in the outermost part of the eyeball and avascular, primarily takes in oxygen from the atmosphere. Previous experimental studies observed corneal edema and neovascularization at simulated altitude of 5500 m for 30 days.[45] In line with this, mice in our study at natural high-altitude environment exhibited evident corneal stroma swelling at 3 days post high-altitude exposure, which was similar with clinical studies.[46] Interestingly, obvious corneal thinning, especially in epithelium and stroma layers, was observed at 40 days acclimatization. This finding was in accordance with the fact that the average corneal thickness of high-land habitants was significantly thinner than those in lowlanders.[47] Related study believed this phenomenon could be accounted for energy supplying alteration during high-altitude adaptation.[45] We found energy supplier glycogen accumulation at corneal epithelium layers confirmed by Periodic Acid–Schiff (PAS) staining at the whole high-altitude exposure (data not shown).

As we know, choroid was mainly composed of macrovascular, middle vascular, and capillary, which made it vulnerable to the impact of angioplerosis regulation. In this study, choroid presented a constant thickening tendency

A

Sample	Name
1	Con Male
2	D1 Male
3	D3 Male
4	D6 Male
5	D10 Male
6	D20 Male
7	D30 Male
8	Con Female
9	D40 Male

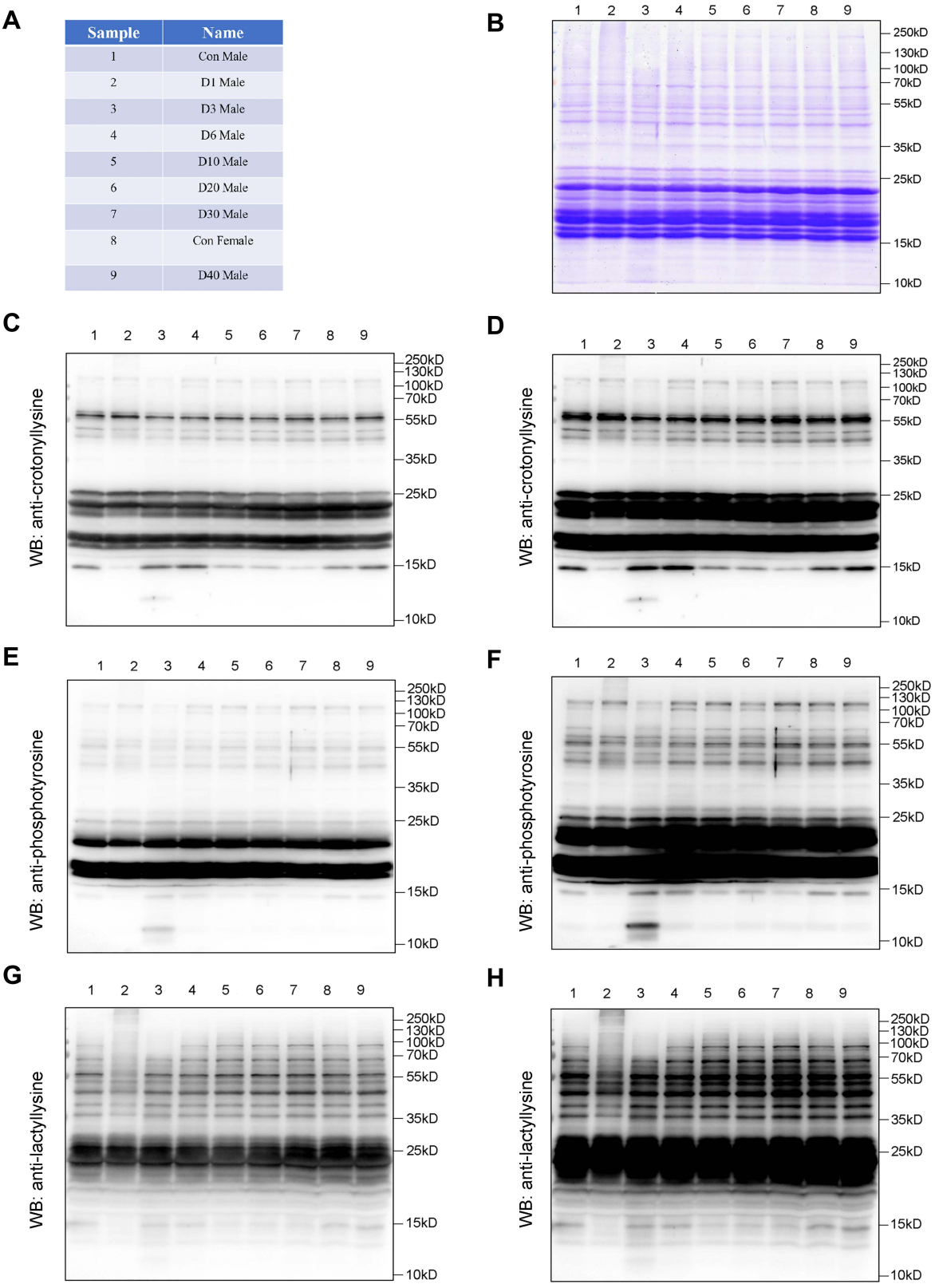

Figure 11 The post-translational modification of ocular tissue at D0 (Control Male), D0 (Control Female) D1, D3, D6, D10, D20, D30, and D40 post high-altitude adaptation. (**A**) The name of each sample. (**B**) The Coomassie brilliant blue staining with gels. (**C**) The expression of lysine crotonylation modification with short exploration. (**D**) The expression of lysine crotonylation modification with long exploration. (**E**) The expression of phosphorylation modification with short exploration. (**F**) The expression of phosphorylation modification with long exploration. (**G**) The expression of lactylation modification with short exploration. (**H**) The expression of lactylation modification with long exploration; N=1.

during high-altitude acclimatation process. We suspected the dilatation of choroidal vessels and capillary bed opening could be related with it. Recently, studies found the choroid thickness was an important index to evaluate the progression of myopia.[48–50] We considered whether an appropriate ocular hypoxia condition could delay the myopia development. In earlier studies, high-altitude retinopathies were observed in experienced climbers, and the manifestations included retinal vascular engorgement, tortuosity, dilation, and hemorrhage.[17,19,51,52] However, no prominent retinal pathological structural changes were observed during the high-altitude exposure. On the one hand, this might be associated with a stronger retinal tolerance ability to high-altitude exposure in mice. On the other hand, we could miss these typical high-altitude induced retinal symptoms for lacking fundus photography, optical coherent tomography (OCT), and fundus angiography detections in vivo.

The ocular tissue of quantitative proteomic analysis provided comprehensive and additional novel information about the regulation of cell stress response-associated proteins during high-altitude acclimatation. Oxidative stress and ferroptosis were common cellular response when encountered with adverse environment and studied in numerous studies.[53,54] We analyzed the proteomic profiles concerning oxidative stress and ferroptosis and found an increase tendency during high-altitude exposure, especially in chronic phase. In addition, to our surprise, the function enrichment analysis found the differential proteins concerning cell stress response during the acute phase of high-altitude exposure were mainly centered on response to radiation and erythrocyte homeostasis. Usually, erythrocytosis was regarded as a chronic high-altitude adaptation response and this finding could provide a new insight on the starting time of erythrocyte stress response.[55] Moreover, radiation was confirmed as a vital disadvantage for ocular cellular response and sunglasses should be equipped with for those who rush entry into high altitude. For chronic phase of high-altitude exposure, we found immune response related pathway and metabolic process pathway changed significantly. Specifically, immune responses, including complement activation, humoral immune response, and leukocyte activation, were strengthened and this could account for an increase of retinal vasculitis and uveitis when living at high altitude for months.

Unfortunately, our proteomic study did not quantify hypoxia-inducible factors (HIFs) and vascular endothelial growth factor (VEGF), the vital moleculars induced by hypoxia. We considered that the expressions were slight and there existed an amplification effect with traditional WB or ELISA detections. Nowadays, post-translational modification (PTM), aroused great attention for enriching the proteins' functional diversity by covalent addition proteins, proteolytic cleavage of subunits. In our study, lysine crotonylation modification, phosphorylation modification, and lactylation modification were detected by pan antibody to explore the potential roles of PTMs on the regulation of high-altitude acclimatization. In the near future, modified proteomics would be applied to fully elucidate the mechanism of molecular cellular stress during high-altitude exposure.

Although our data disclosure the holistic morphological and molecular alterations of ocular tissues following high-altitude exposure, the study inevitably faces some limitation. Firstly, a series of ophthalmological examinations of the ocular tissue of the mice, like electroretinogram, wide-angle fundus photograph, OCT, and angiography, were missing for lack of relative equipment at the high-altitude laboratory. Secondly, since we primarily analyzed from the perspective of the overall protein group changes of ocular tissues, we have not specifically detected the proteomics changes of cornea, lens, vitreous, retina, choroid, and optic nerve, respectively. This may partially ignore valuable ocular components of the molecular regulation mechanism of high-altitude adaption. Thirdly, our experiment lacked a low-altitude control group at the corresponding time points. In the next step, we would focus on specific changes of cornea, retina, and choroid structure, and verify the differential protein-related mechanisms in high-altitude adaptation process.

Conclusion

To our knowledge, this was the first attempt to explore the ocular morphological and systemic proteomic disturbances of mice at natural high-altitude environment. It allowed us to elucidate integrative molecular cell stress and metabolic disorder signatures that have not yet been linked to acute and chronic ocular high-altitude response. The pathological examination data and proteomic data fully displayed the significant impacts of high-altitude environment on the ocular

tissue at least including the cornea, the retina, and the choroid. Altogether, these data could provide a new insight on ocular cellular stress responses to high-altitude exposure.

Data Sharing Statement

The data sets used and analyzed in the present study are available from the corresponding author on reasonable request.

Funding

This work was supported by the National Nature Science Foundation of China (82001484 to P.L.), Natural Science Foundation of China (81900339 to J.H.), the Key projects in Science & Technology Department of Sichuan Province (2018JY0542 to J.H.), and the Fundamental Research Funds for the Central Universities (2682021TPY031 to J.H.).

Disclosure

The authors report no conflicts of interest in this work.

References

1. Betge S, Drinda S, Neumann T, et al. Influence of macitentan on the vascular tone and recruitment of finger capillaries under hypobaric hypoxia in high altitude. *High Alt Med Biol*. 2020;21:336–345. doi:10.1089/ham.2019.0120
2. Sarkar S, Banerjee PK, Selvamurthy W. High altitude hypoxia: an intricate interplay of oxygen responsive macroevents and micromolecules. *Mol Cell Biochem*. 2003;253:287–305. doi:10.1023/A:1026080320034
3. Jha KN. High altitude and the eye. *Asia Pac J Ophthalmol*. 2012;1:166–169. doi:10.1097/APO.0b013e318253004e
4. Dhar P, Sharma VK, Hota KB, et al. Autonomic cardiovascular responses in acclimatized lowlanders on prolonged stay at high altitude: a longitudinal follow up study. *PLoS One*. 2014;9:e84274. doi:10.1371/journal.pone.0084274
5. Willmann G, Gekeler F, Schommer K, Bartsch P. Update on high altitude cerebral edema including recent work on the eye. *High Alt Med Biol*. 2014;15:112–122. doi:10.1089/ham.2013.1142
6. Luks AM, Swenson ER. Evaluating the risks of high altitude travel in chronic liver disease patients. *High Alt Med Biol*. 2015;16:80–88. doi:10.1089/ham.2014.1122
7. Gonzales GF, Tapia V. Increased levels of serum gamma-glutamyltransferase and uric acid on metabolic, hepatic and kidney parameters in subjects at high altitudes. *J Basic Clin Physiol Pharmacol*. 2015;26:81–87. doi:10.1515/jbcpp-2013-0162
8. Kayser B. Nutrition and high altitude exposure. *Int J Sports Med*. 1992;13(1):S129–132. doi:10.1055/s-2007-1024616
9. Zhang W, Jiao L, Liu R, et al. The effect of exposure to high altitude and low oxygen on intestinal microbial communities in mice. *PLoS One*. 2018;13:e0203701. doi:10.1371/journal.pone.0203701
10. Falla M, Papagno C, Dal Cappello T, et al. A prospective evaluation of the acute effects of high altitude on cognitive and physiological functions in lowlanders. *Front Physiol*. 2021;12:670278. doi:10.3389/fphys.2021.670278
11. Algaze I, Phillips L, Inglis P, et al. Incidence of mild cognitive impairment with ascending altitude. *High Alt Med Biol*. 2020;21:184–191. doi:10.1089/ham.2019.0111
12. Wilson MH, Davagnanam I, Holland G, et al. Cerebral venous system and anatomical predisposition to high-altitude headache. *Ann Neurol*. 2013;73:381–389. doi:10.1002/ana.23796
13. Vats P, Singh VK, Singh SN, Singh SB. High altitude induced anorexia: effect of changes in leptin and oxidative stress levels. *Nutr Neurosci*. 2007;10:243–249. doi:10.1080/10284150701722299
14. Davis C, Hackett P. Advances in the prevention and treatment of high altitude Illness. *Emerg Med Clin North Am*. 2017;35:241–260. doi:10.1016/j.emc.2017.01.002
15. Rennie D, Morrissey J. Retinal changes in Himalayan climbers. *Arch Ophthalmol*. 1975;93:395–400. doi:10.1001/archopht.1975.01010020409001
16. Gupta N, Prasad I, Himashree G, D'Souza P. Prevalence of dry eye at high altitude: a case controlled comparative study. *High Alt Med Biol*. 2008;9:327–334. doi:10.1089/ham.2007.1055
17. Bhandari SS, Koirala P, Regmi N, Pant S. Retinal hemorrhage in a high-altitude aid post volunteer doctor: a case report. *High Alt Med Biol*. 2017;18:285–287. doi:10.1089/ham.2017.0003
18. Canepa CA, Harris NS. Ultrasound in austere environments. *High Alt Med Biol*. 2019;20:103–111. doi:10.1089/ham.2018.0121
19. MacCormick IJ, Somner J, Morris DS, et al. Retinal vessel tortuosity in response to hypobaric hypoxia. *High Alt Med Biol*. 2012;13:263–268. doi:10.1089/ham.2011.1097
20. Li M, Tian X, Li X, et al. Diverse energy metabolism patterns in females in Neodon fuscus, Lasiopodomys brandtii, and Mus musculus revealed by comparative transcriptomics under hypoxic conditions. *Sci Total Environ*. 2021;783:147130. doi:10.1016/j.scitotenv.2021.147130
21. de Aquino Lemos V, Antunes HK, Dos Santos RV, Lira FS, Tufik S, de Mello MT. High altitude exposure impairs sleep patterns, mood, and cognitive functions. *Psychophysiology*. 2012;49:1298–1306. doi:10.1111/j.1469-8986.2012.01411.x
22. Ide WW. Central serous chorioretinopathy following hypobaric chamber exposure. *Aviat Space Environ Med*. 2014;85:1053–1055. doi:10.3357/ASEM.4073.2014
23. T. H, Guo H, Shen X, et al. Hypoxia-induced alteration of RNA modifications in the mouse testis and spermdagger. *Biol Reprod*. 2021;105:1171–1178. doi:10.1093/biolre/ioab142
24. Yilmaz A, Ratka J, Rohm I, et al. Decrease in circulating plasmacytoid dendritic cells during short-term systemic normobaric hypoxia. *Eur J Clin Invest*. 2016;46:115–122. doi:10.1111/eci.12416
25. Murray AJ. Energy metabolism and the high-altitude environment. *Exp Physiol*. 2016;101:23–27. doi:10.1113/EP085317

26. Aslam B, Basit M, Nisar MA, Khurshid M, Rasool MH. Proteomics: technologies and their applications. *J Chromatogr Sci*. 2017;55:182–196. doi:10.1093/chromsci/bmw167
27. Kelly RT. Single-cell proteomics: progress and prospects. *Mol Cell Proteomics*. 2020;19:1739–1748. doi:10.1074/mcp.R120.002234
28. Cifani P, Kentsis A. Towards comprehensive and quantitative proteomics for diagnosis and therapy of human disease. *Proteomics*. 2017;17:1600079. doi:10.1002/pmic.201600079
29. Hosp F, Gutiérrez-ángel S, Schaefer MH, et al. Spatiotemporal proteomic profiling of huntington's disease inclusions reveals widespread loss of protein function. *Cell Rep*. 2017;21:2291–2303. doi:10.1016/j.celrep.2017.10.097
30. Chang P, Niu Y, Zhang X, et al. Integrative proteomic and metabolomic analysis reveals metabolic phenotype in mice with cardiac-specific deletion of natriuretic peptide receptor A. *Mol Cell Proteomics*. 2021;20:100072. doi:10.1016/j.mcpro.2021.100072
31. Lee P, Chandel NS, Simon MC. Cellular adaptation to hypoxia through hypoxia inducible factors and beyond. *Nat Rev Mol Cell Biol*. 2020;21:268–283. doi:10.1038/s41580-020-0227-y
32. Majmundar AJ, Wong WJ, Simon MC. Hypoxia-inducible factors and the response to hypoxic stress. *Mol Cell*. 2010;40:294–309. doi:10.1016/j.molcel.2010.09.022
33. Long P, Yan W, Liu J, et al. Therapeutic effect of traditional Chinese medicine on a rat model of branch retinal vein occlusion. *J Ophthalmol*. 2019;2019:9521379. doi:10.1155/2019/9521379
34. Long P, Yan W, He M, et al. Protective effects of hydrogen gas in a rat model of branch retinal vein occlusion via decreasing VEGF-alpha expression. *BMC Ophthalmol*. 2019;19:112. doi:10.1186/s12886-019-1105-2
35. He M, Long P, Yan W, et al. ALDH2 attenuates early-stage STZ-induced aged diabetic rats retinas damage via Sirt1/Nrf2 pathway. *Life Sci*. 2018;215:227–235. doi:10.1016/j.lfs.2018.10.019
36. Li L, Shi L, Yang S, et al. SIRT7 is a histone desuccinylase that functionally links to chromatin compaction and genome stability. *Nat Commun*. 2016;7:12235. doi:10.1038/ncomms12235
37. Huang da W, Sherman BT, Lempicki RA. Systematic and integrative analysis of large gene lists using DAVID bioinformatics resources. *Nat Protoc*. 2009;4:44–57. doi:10.1038/nprot.2008.211
38. Huang da W, Sherman BT, Lempicki RA. Bioinformatics enrichment tools: paths toward the comprehensive functional analysis of large gene lists. *Nucleic Acids Res*. 2009;37:1–13. doi:10.1093/nar/gkn923
39. Szklarczyk D, Gable AL, Nastou KC, et al. The STRING database in 2021: customizable protein-protein networks, and functional characterization of user-uploaded gene/measurement sets. *Nucleic Acids Res*. 2021;49:D605–D612. doi:10.1093/nar/gkaa1074
40. Szklarczyk D, Gable AL, Lyon D, et al. STRING v11: protein-protein association networks with increased coverage, supporting functional discovery in genome-wide experimental datasets. *Nucleic Acids Res*. 2019;47:D607–D613. doi:10.1093/nar/gky1131
41. Chen C, Chen H, Zhang Y, et al. TBtools: an integrative toolkit developed for interactive analyses of big biological data. *Mol Plant*. 2020;13:1194–1202. doi:10.1016/j.molp.2020.06.009
42. Long P, He M, Yan W, et al. ALDH2 protects naturally aged mouse retina via inhibiting oxidative stress-related apoptosis and enhancing unfolded protein response in endoplasmic reticulum. *Aging*. 2020;13:2750–2767. doi:10.18632/aging.202325
43. Toussaint CM, Kenefick RW, Petrassi FA, Muza SR, Charkoudian N:. Altitude, acute mountain sickness, and acetazolamide: recommendations for rapid ascent. *High Alt Med Biol*. 2021;22:5–13. doi:10.1089/ham.2019.0123
44. Dunnwald T, Gatterer H, Faulhaber M, Arvandi M, Schobersberger W. Body composition and body weight changes at different altitude levels: a systematic review and meta-analysis. *Front Physiol*. 2019;10:430. doi:10.3389/fphys.2019.00430
45. Kosaku K, Harada T, Jike T, Tsuboi I, Aizawa S. Long-term hypoxic tolerance in murine cornea. *High Alt Med Biol*. 2018;19:35–41. doi:10.1089/ham.2017.0114
46. Bosch MM, Barthelmes D, Merz TM, et al. New insights into changes in corneal thickness in healthy mountaineers during a very-high-altitude climb to Mount Muztagh Ata. *Arch Ophthalmol*. 2010;128:184–189. doi:10.1001/archophthalmol.2009.385
47. Patyal S, Arora A, Yadav A, Sharma VK. Corneal Thickness in Highlanders. *High Alt Med Biol*. 2017;18:56–60. doi:10.1089/ham.2016.0074
48. Zhang S, Zhang G, Zhou X, et al. Changes in choroidal thickness and choroidal blood perfusion in guinea pig myopia. *Invest Ophthalmol Vis Sci*. 2019;60:3074–3083. doi:10.1167/iovs.18-26397
49. Jin P, Zou H, Zhu J, et al. Choroidal and retinal thickness in children with different refractive status measured by swept-source optical coherence tomography. *Am J Ophthalmol*. 2016;168:164–176. doi:10.1016/j.ajo.2016.05.008
50. Prousali E, Dastiridou A, Ziakas N, Androudi S, Mataftsi A. Choroidal thickness and ocular growth in childhood. *Surv Ophthalmol*. 2021;66:261–275. doi:10.1016/j.survophthal.2020.06.008
51. Mullner-Eidenbock A, Rainer G, Strenn K, Zidek T. High-altitude retinopathy and retinal vascular dysregulation. *Eye*. 2000;14(5):724–729. doi:10.1038/eye.2000.192
52. Bosch MM, Barthelmes D, Landau K. High altitude retinal hemorrhages–an update. *High Alt Med Biol*. 2012;13:240–244.
53. Mao H, Zhao Y, Li H, Lei L. Ferroptosis as an emerging target in inflammatory diseases. *Prog Biophys Mol Biol*. 2020;155:20–28. doi:10.1016/j.pbiomolbio.2020.04.001
54. Kajarabille N, Latunde-Dada GO. Programmed cell-death by ferroptosis: antioxidants as mitigators. *Int J Mol Sci*. 2019;20:4968. doi:10.3390/ijms20194968
55. Haase VH. Regulation of erythropoiesis by hypoxia-inducible factors. *Blood Rev*. 2013;27:41–53. doi:10.1016/j.blre.2012.12.003